Trace gas composition of midlatitude cyclones over the western North Atlantic Ocean: A seasonal comparison of O_3 and CO

O. R. Cooper[1] and J. L. Moody
Department of Environmental Sciences, University of Virginia, Charlottesville, Virginia, USA

D. D. Parrish, M. Trainer, J. S. Holloway, G. Hübler, and F. C. Fehsenfeld
NOAA Aeronomy Laboratory, Boulder, Colorado, USA

Andreas Stohl
Lehrstuhl für Bioklimatologie und Immissionsforschung, Technical University of Munich, Freising, Germany

Received 30 May 2001; revised 4 October 2001; accepted 5 October 2001; published 12 April 2002.

[1] The regional- to synoptic-scale transport of trace gases from North America to the western North Atlantic Ocean (WNAO) is largely controlled by midlatitude cyclones. The four primary airstreams that compose these cyclones, the warm conveyor belt (WCB), cold conveyor belt (CCB), dry airstream (DA), and post cold front (PCF) airstream, exhibit characteristic trace gas mixing ratios that vary seasonally. The present study compares ozone and CO mixing ratios measured in these four airstreams during spring 1996 and late summer/early autumn 1997. The three main influences on this seasonal variation of ozone and CO are surface emissions heterogeneity, photochemistry, and stratosphere/troposphere exchange efficiency. The more southerly springtime cyclone tracks account for nearly 50% of the increase of lower troposphere CO from late summer/early autumn to spring. The remainder of the variation is due to the seasonal cycle of background CO. Stratosphere/troposphere exchange occurs in every DA; however, the seasonal cycle of ozone in the lowermost stratosphere allows greater quantities of ozone to enter the troposphere during spring. Net photochemical ozone production occurs in the late summer/early autumn WCB at all levels and in the lower troposphere PCF. In contrast, springtime net ozone production appears absent from all airstreams, with the CCB influenced by ozone destruction. Ozone and CO are greater in spring, but the relative mixing ratios between airstreams are roughly the same in both seasons. NO_x/CO emissions ratios vary across the midlatitudes according to socioeconomic factors. It is expected that the emissions variation influences the ozone production efficiency of the cyclone airstreams that draw from these regions. *INDEX TERMS:* 0368 Atmospheric Composition and Structure: Troposphere—constituent transport and chemistry; 0322 Atmospheric Composition and Structure: Constituent sources and sinks; 0345 Atmospheric Composition and Structure: Pollution—urban and regional (0305); 3364 Meteorology and Atmospheric Dynamics: Synoptic-scale meteorology; *KEYWORDS:* cyclone, pollution, transport, chemistry, stratospheric intrusions, airstreams

1. Introduction

[2] The North Atlantic Regional Experiment (NARE) is a multi-institutional, multiyear research initiative with the primary goal of understanding the oxidizing capacity and radiative balance of the atmosphere [*Fehsenfeld et al.*, 1996]. NARE has focused its research on the ozone budget of the temperate North Atlantic Ocean, a region that receives anthropogenic emissions from the surrounding continents but is not a significant source itself. The North Atlantic is therefore an ideal location to study trace gas lifetime and transformation. A specific goal of NARE is to determine the meteorological mechanisms that transport trace gases from North America to the western North Atlantic Ocean (WNAO). NARE studies initially focused on the low-level outflow within the warm sector of midlatitude cyclones as the primary transport mechanism [*Berkowitz et al.*, 1996; *Merrill and Moody*, 1996; *Moody et al.*, 1996]. Other NARE studies [*Berkowitz et al.*, 1995; *Merrill et al.*, 1996; *Moody et al.*, 1996; *Oltmans et al.*, 1996; *Parrish et al.*, 2000], and several studies from the Atmosphere Ocean Chemistry Experiment (AEROCE) [*Moody et al.*, 1995; *Cooper et al.*, 1998; *Prados et al.*, 1999], have examined the transport of ozone from the upper troposphere and lower stratosphere to the WNAO, subsiding isentropically along the western side of midlatitude cyclones. More recently, *Cooper et al.* [2001a] identified a variety of individual airstreams within midlatitude cyclones of the WNAO and determined the associated trace gas signatures. They found that the warm sector was not the only portion of a cyclone that exports significant amounts of anthropogenic emissions to the WNAO.

[3] While the literature contains many case studies of trace gas transport to the WNAO, a comprehensive analysis of in situ measurements is required in order to discern the typical trace gas signatures of midlatitude cyclones, the synoptic-scale features responsible for the bulk of trace gas export from North America. In response to this need, *Cooper et al.* [2002] (hereinafter referred to as C2002) developed a conceptual model of a midlatitude cyclone tracking from North America to the WNAO, highlighting

[1]Now at NOAA Aeronomy Laboratory, Boulder, Colorado, USA.

0148-0227/02/2001JD000902$09.00

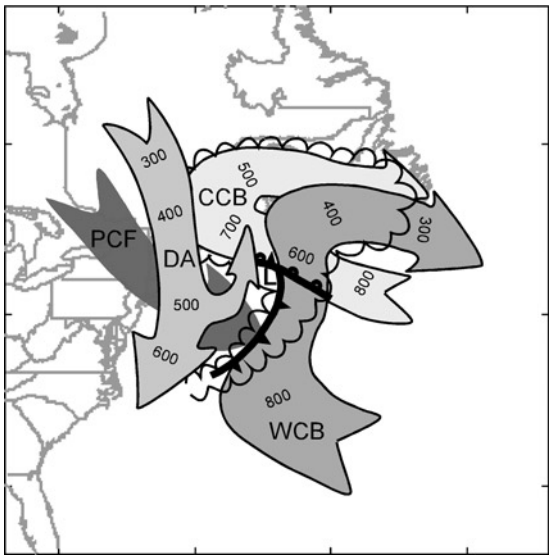

Figure 1. Model of a midlatitude cyclone showing the warm conveyor belt (WCB), cold conveyor belt (CCB), dry airstream (DA), and post-cold-front airstream (PCF). The center of the cyclone is indicated (L) and the scalloped lines indicate the border of the comma cloud formed by the airstreams. The numbers on the warm and cold conveyor belts indicate the pressure at the top of these airstreams, while the numbers on the dry airstream indicate the pressure at the bottom of this airstream. The PCF flows beneath the dry airstream. The cyclone location on the map is typical of springtime. (After *Carlson* [1980, Figure 9], *Bader et al.* [1995, Figures 3.1.24 and 3.1.27b], and *Cooper et al.* [2001a, Figure 2].)

the typical chemical composition of the cyclone's airstreams. The model is a composite of chemical and meteorological data collected on 11 flights above the Canadian Maritimes during the September 1997 NARE campaign. Four basic types of cyclone airstreams were analyzed, the warm conveyor belt (WCB), cold conveyor belt (CCB), dry airstream (DA), and post cold front (PCF) airstream. The meteorological and chemical characteristics of these airstreams are discussed in detail elsewhere [*Carlson*, 1980; *Browning and Monk*, 1982; *Browning and Roberts*, 1994; *Bader et al.*, 1995; *Carlson*, 1998; *Cooper et al.*, 2001a, 2002], but an idealized representation of their structure is presented in Figure 1.

[4] The C2002 study showed that late summer/early autumn characteristic mixing ratios, such as the mean or median, could be established for the various cyclone airstreams using data from several flights. These characteristic mixing ratios are influenced by (1) meteorological processes within the cyclone and (2) surface emissions heterogeneity. The meteorological processes are expected to have similar influences on trace gases for any cyclone tracking from North America to the WNAO; for example, stratosphere/troposphere exchange within the DA will enhance ozone in the middle and upper troposphere; wet deposition within the WCB and CCB will prevent most NO_y from being exported to the free troposphere. In contrast, surface emissions heterogeneity can cause interannual variation of the characteristic mixing ratios. For example, a year in which cyclones track close to the populated east coast of North America results in higher median mixing ratios of anthropogenic emissions within airstreams than a year in which cyclones track farther out to sea. However, C2002 propose that seasonal relationships between trace gases, such as the ozone/CO slope, vary less from year to year. Therefore these relationships are a more robust chemical signature of airstreams than mean or median mixing ratios.

[5] The cyclone conceptual model developed by C2002 was based on a composite cyclone from late summer/early autumn. The purpose of the present study is to expand the conceptual model to include a springtime composite cyclone based on chemical and meteorological data from the NARE 1996 intensive above the eastern United States and WNAO. Three factors influenced the seasonal variation of airstream trace gas signatures: (1) surface emissions heterogeneity: springtime cyclones follow a more southerly path than their late summer/early autumn counterparts, spending more time over the high- emission regions of North America; (2) meteorological processes: STE is more efficient in spring, resulting in enhanced ozone in the DA and in background air; (3) photochemistry: diminished photochemical activity, relative to late summer/early autumn, in winter and early spring allows an accumulation of CO and ozone in the troposphere. Additionally, consideration must be given to outbreaks of peroxy acetyl nitrate (PAN) from the polar regions into midlatitudes which contributes to photochemical ozone production, and to fresh emissions at low sunlight levels, which may lead to net ozone destruction in some airstreams.

[6] This manuscript continues in section 2 with a brief description of the chemical and meteorological data used in the study. This section also describes the method by which the springtime composite cyclone was constructed. Section 3 compares the spring and late summer/early autumn composite cyclones in terms of storm tracks, ozone, CO, and the ozone/CO relationship. These results are then compared to a major summertime pollution episode in section 4. Finally, we summarize the results in section 5 and draw attention to the relevance and applications of composite cyclones.

2. Method

[7] This manuscript presents data from the NARE'96 (20 March to 11 April 1996) and NARE'97 (6 September to 2 October 1997) aircraft intensives. The methodologies used to analyze these data are presented by *Cooper et al.* [2001a, 2002]. As with the NARE'97 study, the NARE'96 chemical data were measured from the NOAA WP-3D Orion aircraft, between the surface and 8 km above sea level. Figure 2 shows the tracks of the 13 NARE'97 flights, from St. John's, Newfoundland, and the nine NARE'96 flights from Providence, Rhode Island (transit flights to and from Tampa, Florida, are included).

[8] A variety of chemical species was measured during both campaigns, but this study focuses on ozone and CO. The data were collected at 1-s time resolution, which at the speed of the aircraft corresponds to an average over ~0.1 km of flight path. The respective ozone and CO measurement techniques were similar in 1996 and 1997, with similar accuracy and precision [*Cooper et al.*, 2002]. Table 1 shows the number of airstreams sampled during each season and the number of 1-s data measurements with both ozone and CO values. This type of study requires data from as many airstreams as possible, but we are limited by the number of events sampled during the NARE campaigns. However, the NARE databases provide the highest number of samples available for the eastern United States and WNAO, and we believe that most airstreams were adequately sampled in order for us to characterize their chemical signatures. Typically, three-eight airstreams were intersected in each of the three layers of the troposphere (Table 1). The only airstream that we believe to be inadequately sampled was the midtroposphere CCB during NARE'97. Just two CCBs were sampled in the midtroposphere, with a relatively small number of data points (1102).

[9] Back trajectories were one of the tools used to identify individual airstreams. Three-dimensional 120-hour air mass back trajectories were calculated at every measurement point along the NARE'96 flight tracks with the FLEXTRA (V3.2) trajectory model [*Stohl et al.*, 1995; *Stohl and Seibert*, 1998]. FLEXTRA

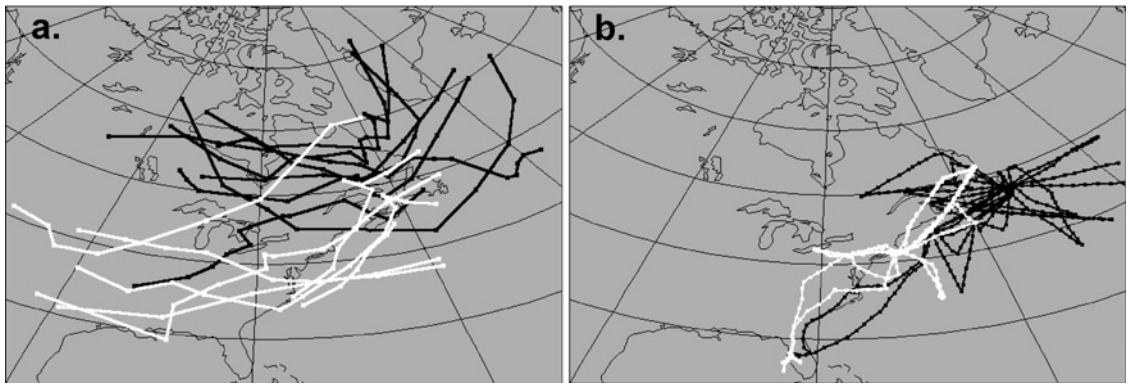

Figure 2. (a) Spring 1996 (white lines) and late summer/early autumn 1997 (black lines) cyclone tracks. (b) Spring 1996 (white lines) and late summer/early autumn 1997 (black lines) flight tracks.

was driven every 6 hours by analysis fields and every other 3-hour by 3-hour forecast fields from the European Centre for Medium-Range Weather Forecasts [*ECMWF*, 1995] with grid spacing of 1° longitude × 1° latitude. The model uses bicubic horizontal, quadratic vertical, and linear time interpolation. No isentropic assumption is invoked, which is important especially for ascending airstreams, where condensation violates this assumption.

[10] The NARE'96 aircraft chemical data were grouped according to the airstream they occupied, using the same methods to identify airstreams as the NARE'97 study [*Cooper et al.*, 2001a, 2002]. For example, seven of the nine flights intersected the dry airstreams of seven individual midlatitude cyclones. The chemical data from these seven dry airstreams were amalgamated and, for the remainder of this analysis, are considered representative of the range of ozone and CO mixing ratios typically found in springtime dry airstreams. To briefly summarize, the airstreams analyzed were the WCB, CCB, DA, and PCF, partitioned into three levels, the lower (<2 km above sea level (asl)), middle (>2 km asl and <6 km asl), and upper troposphere (>6 km asl). The DA did not penetrate to the altitudes of the lower troposphere; similarly, the CCB and PCF did not penetrate to the altitudes of the upper troposphere.

[11] The ratio of ozone mixing ratio to isentropic potential vorticity (IPV) was calculated at the tropopause within the DA of each cyclone. Ozone was measured by ozonesondes launched daily from Sable Island, Nova Scotia (44°N, 60°W), during NARE'97 and from Charlottesville, Virginia (38°N, 78°W), during NARE'96. The balloon-borne ozonesondes were equipped with the widely used and tested electrochemical concentration cell (ECC) O_3 sensor [*Komhyr*, 1969; *Komhyr et al.*, 1995], according to the procedures of *Oltmans et al.* [1996]. The ozonesondes produced vertical profiles of ozone, temperature, and frost point between the surface and ~35 km asl. The data were partitioned into 0.25 km vertical layers and reported as layer averages. IPV was calculated from three-dimensional meteorological fields generated by the National Centers for Environmental Prediction (NCEP) Eta Data Assimilation System (EDAS), obtained from the Data Support Section archive at the National Center for Atmospheric Research (NCAR) Scientific Computing Division (SCD). These analyses fields were available every 3 hours, on 25 constant pressure surfaces between 1000 and 50 hPa. The 40-km horizontal grid spacing is based on the AWIPS grid 212. The tropopause was defined as the region of atmosphere between the 1 and the 2 pvu (potential vorticity unit, 1 pvu = 1×10^{-6} m^2 K kg^{-1} s^{-1}) isosurfaces. While the Eta model data are of high quality, the calculated IPV at a given location is not so accurate as the in situ ozone data measured by the ozonesondes. However, we are using the ozone/IPV ratio to determine the broad seasonal variation of ozone in the lowermost stratosphere, and the calculated IPV is adequate for our purposes.

[12] Linear regression lines, of the form $y = mx + b$, were determined using the two-sided method. The commonly used linear least squares regression assumes deviations from a linear relationship due to deviations in the dependent variable only (y). However, in this study both CO and ozone contribute to the deviations. The two-sided regression method accounts for both the dependent and the independent deviations [*Press et al.*, 1992; *Parrish et al.*, 1998]. For this procedure the data were weighted by the inverse of the square of the approximate measurement precision: 1 ppbv for ozone and 1 ppbv for CO. The absolute value of the slopes (m) of the two-sided regressions were usually significantly greater than those from the common linear least squares regressions.

[13] Figure 3 displays "background" mixing ratio values of ozone and CO as reference points for the range of mixing ratios shown for each airstream. The late summer/early autumn background O_3 value of 43 ppbv was determined from measurements of unpolluted air in the lower troposphere at Niwot Ridge, Colorado, averaged over the months of August–October [*Parrish et al.*, 1986]. Similarly, the spring background ozone value is 48 ppbv, the average over March and April. The late summer/early autumn background CO value of 79 ppbv is the average of the free tropospheric CO measurements during NARE'97 minus the standard deviation; the spring background CO value is 115 ppbv, as similarly determined from the NARE'96 data.

Table 1. Sample Size of Each Airstream

	Number of Airstreams Sampled / Number of Data Points		
	Lower Troposphere	Midtroposphere	Upper Troposphere
		NARE'96	
DA		7/21721	6/14798
WCB	3/7856	8/9980	7/9944
CCB	3/14684	3/20417	
PCF	7/44733	8/7946	
		NARE'97	
DA		7/28777	5/8804
WCB	8/41714	11/65329	9/17007
CCB	4/15120	2/1102	
PCF	7/28608	6/7578	

3. Comparison of Spring and Late Summer/Early Autumn Composite Cyclones

3.1. Seasonal Shift of Cyclone Tracks

[14] Midlatitude cyclones tracked across the eastern United States during the spring NARE'96 study period and across eastern Canada during the late summer/early autumn NARE'97

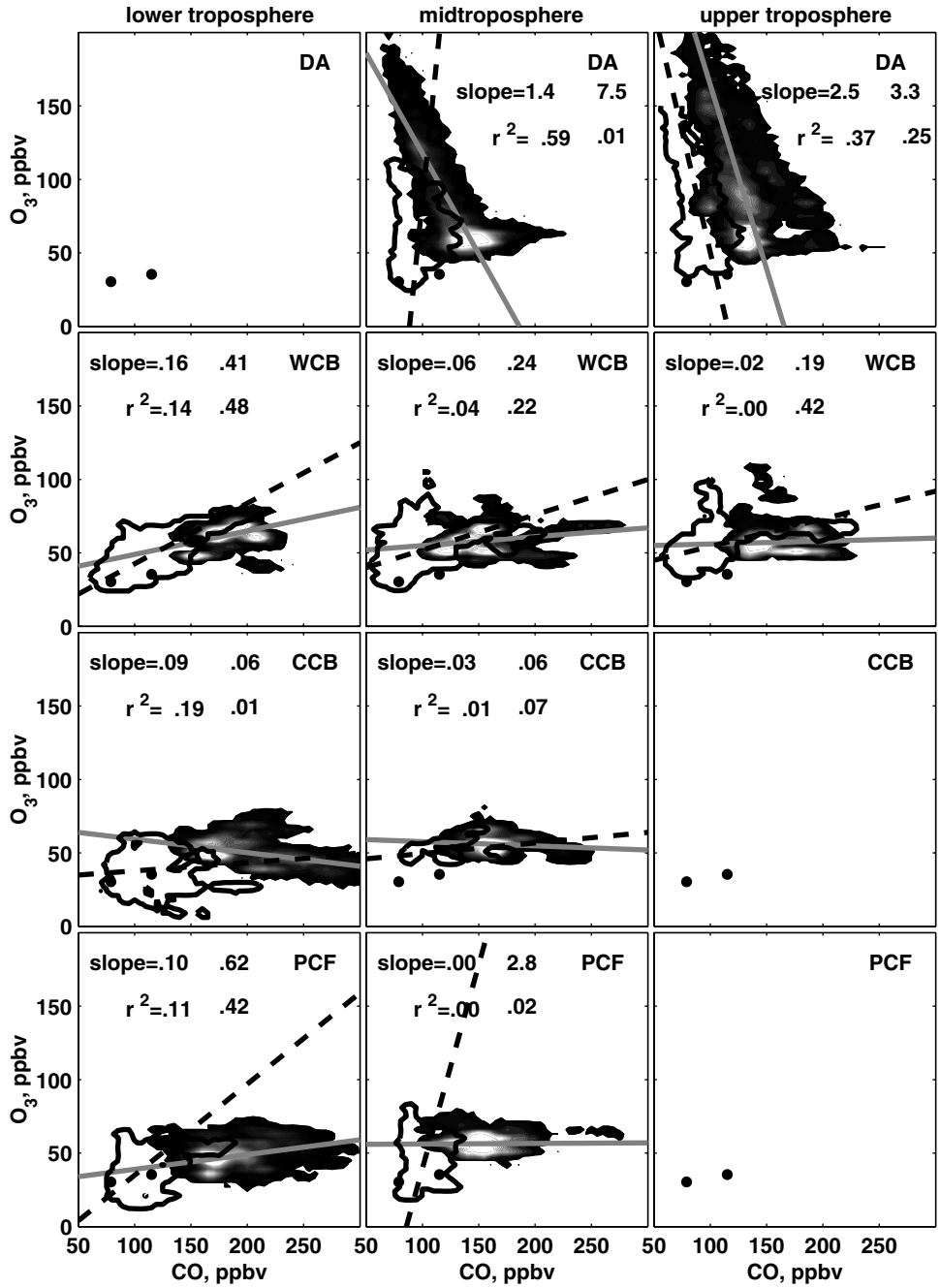

Figure 3. Spring 1996 ozone versus CO for all four airstreams at three levels of the troposphere. The lighter (darker) shading corresponds to relatively higher (lower) data density. The range of the late summer/early autumn 1997 data for each airstream is outlined in red. The linear regression lines for each airstream are shown for spring 1996 (gray lines) and late summer/early autumn 1997 (red dashed lines), with the slope and *r*-squared values labeled in black (spring) and red (late summer/early autumn). Ozone and CO background mixing ratios are shown for spring (blue dot) and late summer/early autumn (green dot). See color version of this figure at back of this issue.

study period (Figure 2a). Accordingly, the springtime research flights were conducted at more southerly latitudes in order to intercept the cyclones (Figure 2b). This seasonal shift of the cyclone tracks agrees with the results of a recent 1-year "climatology" of airstream in the Northern Hemisphere [*Stohl*, 2001]. During the period April 1997 to April 1998 the inflow regions of WCBs was south of 50°N during summer and autumn but south of 40°N during winter and spring. Comparison of the cyclone tracks (Figure 2) to the CO emissions map (Figure 4) shows the springtime cyclones are much more likely to encounter widespread anthropogenic CO source regions. Figure 5 shows the paths of the back trajectories associated with each sampled air stream for the NARE'96 study. The overwhelming majority of back trajectories associated with the lower troposphere airstreams pass over the major CO emission regions. This is true even of the springtime cyclones that formed off Cape Hatteras and traveled over the ocean, parallel to the coast. In contrast, the corresponding late summer/early autumn back trajectories have a stronger association with the low-emission regions of the WNAO and the sparsely populated regions of Canada [cf. *Cooper et al.*, 2002,

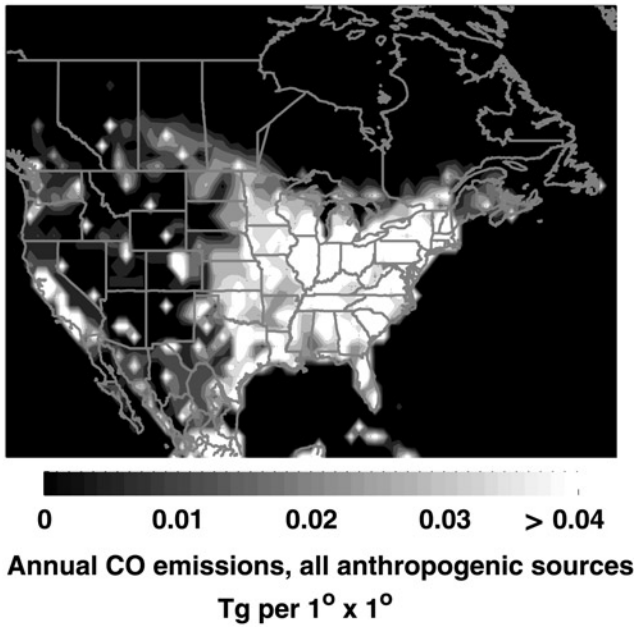

Figure 4. Annual CO emissions from all North American anthropogenic sources. Data are at $1^\circ \times 1^\circ$ resolution and based on a 1990 emissions inventory [*Olivier et al.*, 1999].

Figure 6]. As discussed below, the seasonal shift of the cyclone tracks, coupled with surface emissions heterogeneity, has a strong impact on airstream trace gas signatures.

3.2. CO

[15] Diminished oxidation by the OH radical results in greater tropospheric background CO mixing ratios in spring. *Novelli et al.* [1998] report springtime values ~80% greater than during autumn at Northern Hemisphere surface background monitoring sites. This seasonal CO difference is clearly evident in the NARE data (Table 2). Figure 6 shows mean vertical CO profiles for each airstream in spring and late summer/early autumn. Spring values are ~80% greater in the lower troposphere, similar to the surface seasonal variation observed by *Novelli et al.* [1998], and 40–50% greater in the middle and upper troposphere.

[16] By determining the seasonal increase of the background CO mixing ratio, from late summer/early autumn to spring, we can determine the contribution of surface emissions heterogeneity to the seasonal increase of CO within individual airstreams. For a given season we define the background CO mixing ratio as the mean of all free troposphere CO measurements (4.5–8 km asl), minus the standard deviation. This yields background CO mixing ratios of 79 and 115 ppbv for late summer/early autumn and spring, respectively, and a 36 ppbv increase in background CO from late summer/early autumn to spring. CO mixing ratios of the lower troposphere airstreams are ~80 ppbv greater in spring. Therefore nearly half (36 ppbv) of the springtime enhancement in the lower troposphere airstreams is due to the seasonal background cycle, and the remainder is due to the cyclones tracking across regions with greater CO emissions. Likewise, greater influence from regions of high CO emissions during spring produces an additional 15 ppbv in the midtroposphere PCF and an additional 11 and 17 ppbv in the middle and upper troposphere WCB, respectively.

3.3. Ozone

[17] As with CO, tropospheric ozone also peaks in springtime. The cause of the spring ozone maximum, common to many locations and regions of the troposphere is a topic that receives great attention in the literature. The various explanations are reviewed and discussed at length by *Monks* [2000]. The debate centers around how much of the ozone maximum is the result of stratosphere/troposphere exchange (STE) and how much is the result of photochemical ozone production. In terms of STE, mass transport from the stratosphere to the troposphere in the Northern Hemisphere is believed to be at a maximum in late spring and a minimum in autumn [*Appenzeller et al.*, 1996]. The excess mass transfer coupled with greater ozone mixing ratios in the stratosphere during spring leads to a springtime maximum of ozone transport into the troposphere. In terms of photochemistry, the wintertime buildup of ozone precursors, such as peroxy acetyl nitrate (PAN), is a major factor. In spring the relatively high precursor concentrations lead to photochemical ozone production in the free troposphere [*Penkett and Brice*, 1986]. The springtime production of ozone in addition to the increased lifetime of ozone in winter and spring would contribute to the springtime ozone maximum [*Liu et al.*, 1987].

[18] Table 2 and Figure 6 show that ozone is greater in the spring for all airstreams throughout the troposphere, although the enhancement is not uniform. The springtime enhancements are greatest in the lower troposphere, the result of the general increased background ozone mixing ratios [*Logan*, 1999] and a shift in air mass source region. Back trajectories indicate that the continental United States serves as a major source region for the lower troposphere airstreams during spring, while central Canada and the WNAO are the major source regions during late summer/early autumn. Surface background ozone over the United States is 10–20 ppbv greater in spring than over the WNAO and central Canada in autumn [*Logan*, 1999]. The median springtime mixing ratio and springtime enhancement are greater in the WCB than the CCB or PCF in the lower troposphere. This is because the WCB has a stronger association with the continental United States than the other two airstreams, and ozone production efficiency may also play a role as discussed below.

[19] The DA has the greatest ozone median in the middle and upper troposphere in both seasons (Table 2), due to STE occurring within the DA. The greater springtime median is the result of the seasonal ozone cycle in the Northern Hemisphere stratosphere. Most stratospheric ozone is produced at low latitudes and subsequently transported to high latitudes. During the dark winter months, ozone builds up in the polar stratosphere. During summer the poleward ozone transport is weaker and the near-constant daylight allows naturally occurring NO_x to destroy ozone in the polar stratosphere. As a result, column ozone in the Northern Hemisphere stratosphere reaches a minimum in September with a springtime maximum [*Fahey and Ravishankara*, 1999]. Because the DA always draws from the polar side of the upper level polar front, a STE event in the spring would introduce more ozone to the troposphere than an event of equal strength in late summer/early autumn. The ozone/IPV ratio at the tropopause, within the DA, is an indicator of the relative amount of ozone in the lowermost stratosphere available for STE. The ozone/IPV ratio was 72 ppbv/pvu in the springtime study region, and 42 ppbv/pvu in the late summer/early autumn study region. While the ozone/IPV ratio increased by 71% from late summer/early autumn to spring, the median ozone mixing ratio of the upper troposphere DA only increased by 12% due to dilution of the stratospheric air with upper tropospheric air.

3.4. O_3/CO Relationship

[20] The ozone/CO relationship can be used as an indicator of photochemical activity. The typical positive slope found in emission regions during summer indicates net ozone production, while a negative slope during winter indicates a net ozone loss [*Parrish et al.*, 1998, 1999]. However, the effects of transport on the relationship should be considered before conclusions are drawn about ozone production efficiency. *Chin et al.* [1994] found that

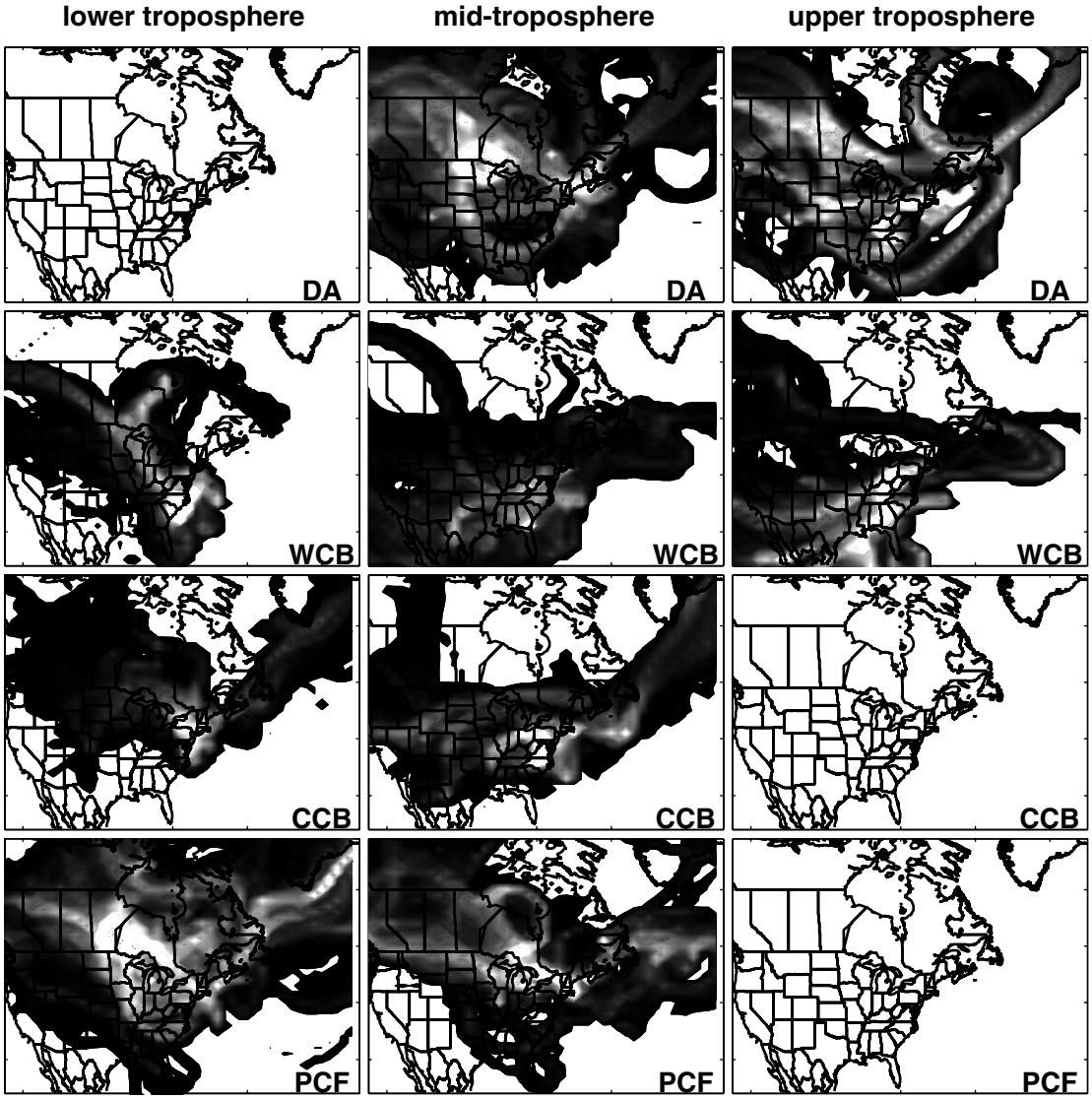

Figure 5. Paths of back trajectories associated with each airstream. The trajectories were initialized along the NARE'96 flight tracks and extend five days back in time. Lighter (darker) shading indicates a greater (lesser) number of trajectories passed through each $1^\circ \times 1^\circ$ grid square. For clarity, only those grid squares with more than two trajectory points are shaded (trajectory points are calculated every 6 hours). These plots are not analogous to the probability density trajectory plots that have appeared elsewhere [*Moody et al.*, 1998; *Cooper and Moody*, 2000].

aged air masses at rural sites in eastern North America exhibit an ozone/CO slope of 0.3. *Cooper et al.* [2001b] showed that transport of air masses from widely varying source regions plays a major role in maintaining the 0.3 slope at a rural location. Similarly, the ozone/CO slopes reported in this study are the result of trace gas signatures from different source regions; for example, the WCB draws from both the relatively clean marine boundary layer and the polluted continental mixed layer. Ozone pollution episodes occur in air masses that have spent several days over the continent and are not usually of recent marine origin [*Comrie and Yarnal*, 1992; *Comrie*, 1994; *Cooper and Moody*, 2000]. These episodes occur on the western side of surface anticyclones, which are also the regions where ozone of stratospheric origin is most likely to mix down to the surface [*Cooper and Moody*, 2000]. In contrast, the stable marine boundary layer receives less ozone from the free troposphere, while halogen and OH chemistry destroy ozone [*Penkett et al.*, 1997; *Galbally et al.*, 2000]. Therefore the background mixing ratios of the marine boundary layer may not necessarily correspond to the background mixing ratios over the continent, and a regression line fit through a scatterplot of ozone versus CO from air masses of marine and continental origin will not necessarily give a true representation of ozone production efficiency.

[21] Bearing in mind the strong influence of transport, the ozone/CO relationship has been shown to be a more robust chemical signature of cyclone airstreams than the median ozone or CO mixing ratios [*Cooper et al.*, 2002]. Median mixing ratios vary depending on airstream origin and the trace gas emissions associated with these source regions. However, the slope of the ozone/CO relationship remains fairly constant, regardless of the frequency with which various source regions influence a particular type of airstream.

[22] Figure 3 displays ozone versus CO for spring 1996 and late summer/early autumn 1997, for each airstream in the lower, middle, and upper troposphere. The most apparent difference between the two seasons is that ozone and CO mixing ratios are much lower in late summer/early autumn, for reasons discussed above. Closer inspection reveals seasonal differences of the ozone/CO slopes. In the lower troposphere the WCB and PCF exhibit

Table 2. Median Values of CO and Ozone by Airstream, Including the Difference Between 1996 Spring and 1997 Late Summer/Early Autumn Values[a]

	Lower Troposphere, 0–2 km asl			Midtroposphere, 2–6 km asl			Upper Troposphere, >6 km asl		
	Spring 1996	Autumn 1997	Spring 1996 to Autumn 1997	Spring 1996	Autumn 1997	Spring 1996 to Autumn 1997	Spring 1996	Autumn 1997	Spring 1996 to Autumn 1997
					CO, ppbv				
All	174	102	72	143	96	47	136	93	43
DA	–	–	–	135	96	39	128	90	38
WCB	176	97	79	140	93	47	146	93	53
CCB	184	101	83	159	120	39	–	–	–
PCF	176	98	78	151	100	51	–	–	–
					Ozone, ppbv				
All	49	40	9	58	52	6	62	59	3
DA	–	–	–	62	56	6	85	76	9
WCB	63	42	21	58	52	6	57	54	3
CCB	50	38	12	56	50	6	–	–	–
PCF	48	33	15	57	46	11	–	–	–

[a] "All" refers to all data measured from the WP-3D aircraft during the study period.

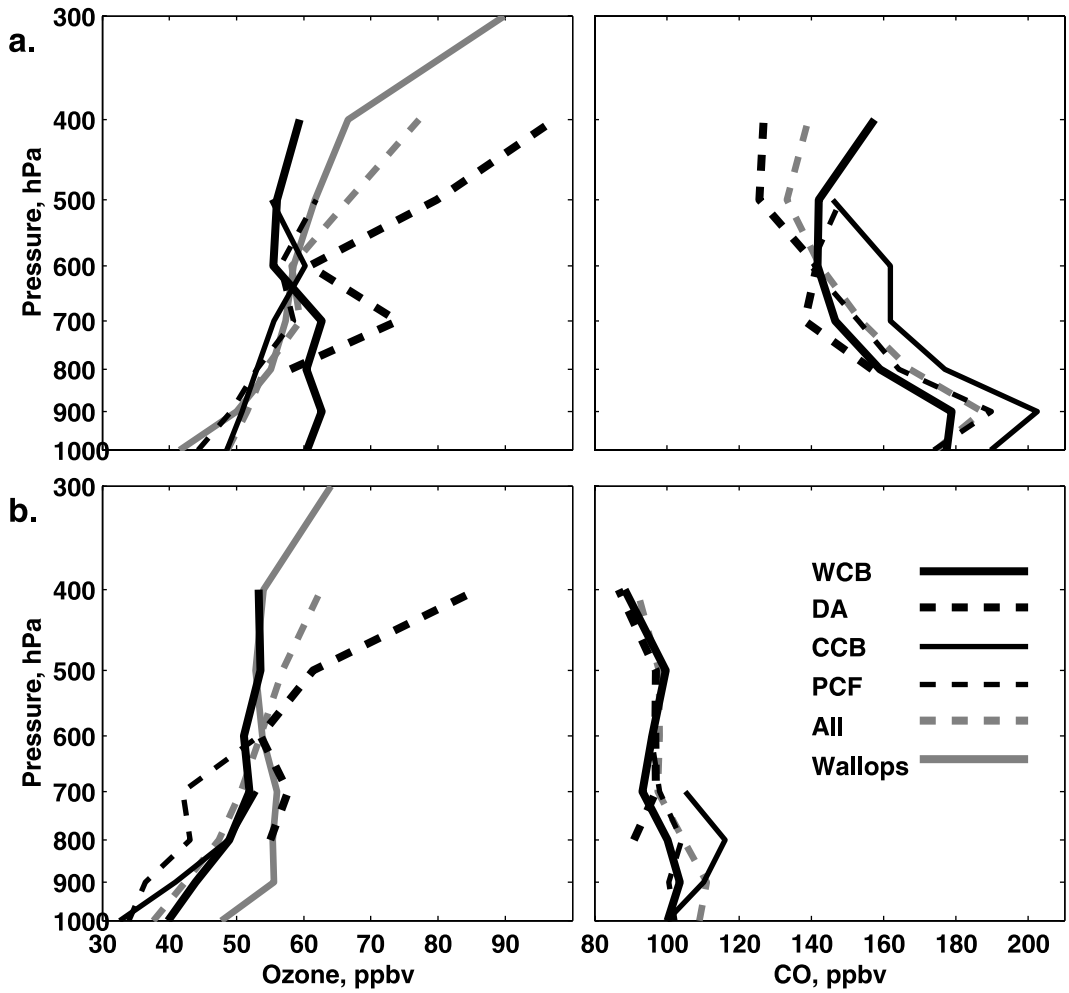

Figure 6. Mean ozone and CO vertical profiles for a) spring 1996 and b) late summer/early autumn 1997. The data were partitioned into 100 hPa bins for the WCB (thick solid line), DA (thick dashed line), CCB (thin solid line) and PCF (thin dashed line) airstreams. The mean profile (gray dashed line) for all of the aircraft data is also shown, as are the a) March–April and b) September mean ozone profiles (gray solid line) for Wallops Island, VA [data from *Logan*, 1999].

positive slopes in both seasons, but the slopes are smaller in spring, and the *r*-squared values indicate that the regression lines explain much less of the variance. These slopes are smaller during the spring for several reasons. First, compared to the background mixing ratios for each season, these data show less net ozone production in spring. This process lowers the right-hand side of the regression line during spring. Second, the springtime lower troposphere WCB experiences less ozone destruction; that is, of the marine boundary layer air masses that influence the WCB, those from late summer/early autumn spend a longer time in the marine boundary layer, allowing for greater ozone destruction, while those from spring have a recent continental origin (Figure 5) and therefore experience less ozone destruction. Finally, the PCF has a northerly origin in both seasons, but background ozone in the lower troposphere of the Canadian high latitudes is much less in late summer/early autumn than during spring [*Logan*, 1999]. These last two processes raise the left-hand side of the regression lines during spring.

[23] For both seasons the slope of the PCF decreases in the midtroposphere, explaining an insignificant portion of the variance. In the WCB the late summer/early autumn slope decreases in the middle and upper troposphere but still explains >20% of the variance, while the spring slope is virtually zero in the middle and upper troposphere, explaining insignificant portions of the variance.

[24] The lower troposphere CCB has virtually no slope in late summer/early autumn and a slightly negative slope in spring, explaining 19% of the variance. Thus polluted events in the cloudy CCB are associated with no net ozone production in late summer/early autumn and ozone destruction in spring. The CCB shows no significant slopes in the midtroposphere for either season.

[25] The midtroposphere DA has a positive but insignificant slope during late summer/early autumn; the influence of STE is evident from the ozone values greater than 75 ppbv. However, during spring the midtroposphere DA has a robust negative slope due to STE events penetrating deeper into the troposphere. Both seasons have a slope of approximately −3 in the upper troposphere.

4. Comparison to Summer Pollution Episode

[26] The present study has focused on the comparison of spring and late summer/early autumn data above the WNAO, the two seasons that roughly coincide with the seasonal maximum and minimum of tropospheric background ozone and CO. However, none of the analyzed cyclones contained a major pollution episode comparable to those that occur during summer over the eastern United States. To illustrate the differences and similarities between the conceptual cyclone model and a major summertime pollution episode, we compare the present results to NARE measurements over the WNAO on August 28, 1993 [*Buhr et al.*, 1996].

[27] The NCAR King Air aircraft flew eastward from Portland, Maine (44° N, 70° W), at 1100 UTC, August 28, sampling the marine boundary layer on the outbound leg and the middle and upper troposphere (up to 6 km asl) on the return leg; the flight ended by 1830 UTC (Figure 7). Concurrently, a midlatitude cyclone was tracking eastward across Quebec, its cold front approaching the WNAO from the east, placing the flight track in the cyclone warm sector. The warm sector formed one day earlier over the continent on the northwest side of a surface anticyclone, which had remained stationary above the eastern United States and WNAO over the previous five days. The pollution episode was exacerbated by the hot, stagnant conditions associated with the western side of the anticyclone, a common occurrence during summer over the eastern United States [*Comrie and Yarnal*, 1992; *Comrie*, 1994; *Cooper and Moody*, 2000]. The region of the warm sector sampled by the aircraft was ahead of the WCB cloud band, so technically, the WCB was not sampled (Figure 7a). However, stationary surface sites show that during this type of

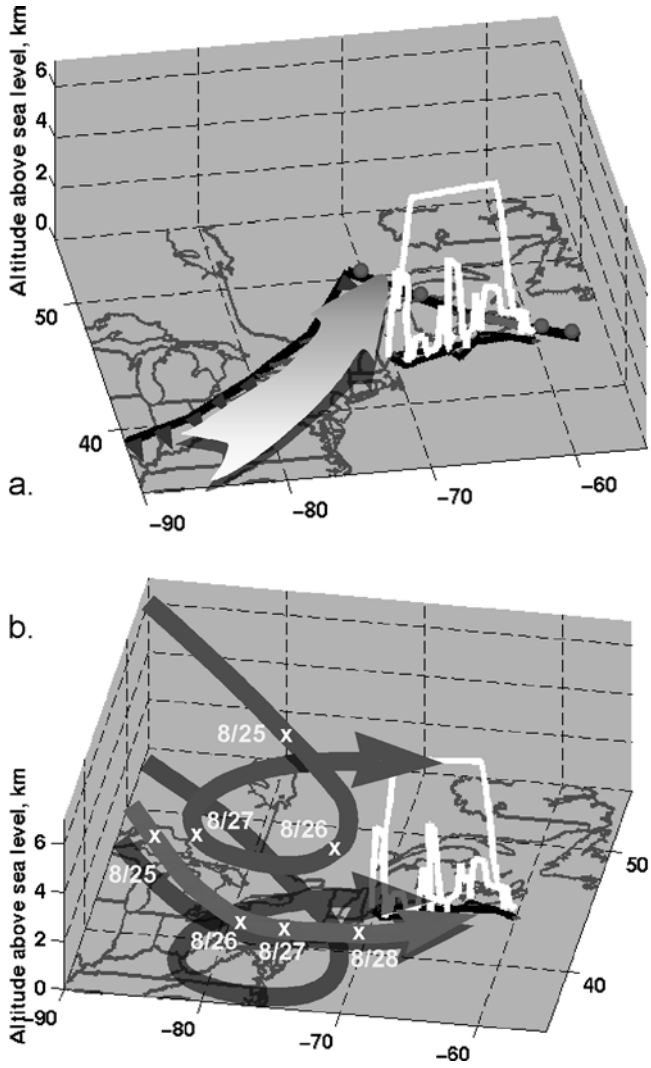

Figure 7. (a) Location of cold and warm fronts, 1200 UTC, 28 August 1993. Flight track is shown in white and the rising green arrow represents the WCB. (b) Back trajectories showing the path of the anthropogenic influenced air mass (red) and stratospheric influenced air mass (blue). The trajectories arrived over the WNAO at 1800 UTC, 28 August; the month and day (m/dd) of the trajectory points at 0000 UTC are shown in white. See color version of this figure at back of this issue.

event, ozone mixing ratios are as great in the WCB as the rest of the warm sector and do not decrease until the cold front has passed and the PCF advects relatively clean air from the NW [*Cooper and Moody*, 2000; *Cooper et al.*, 2001b]. We therefore assume that ozone and CO mixing ratios within the lower troposphere WCB would have been comparable to those measured in the rest of the warm sector.

[28] Figure 8 shows ozone versus CO from this flight as 5-s averages between 1500 and 1830 UTC, highlighting data in the lower, middle, and upper troposphere. Ozone and CO reached as high as 140 and 360 ppbv, respectively, in the lower troposphere, far greater than any mixing ratios measured in the lower troposphere during spring 1996 or late summer/early autumn 1997. Back trajectories indicate that this polluted air mass traveled within the lower troposphere across the upper Midwest and eastern United States and out to the WNAO over the previous four days (Figure 7b); 18–24 hours elapsed between the time the air mass left the east coast and reached the sampling location. Even though

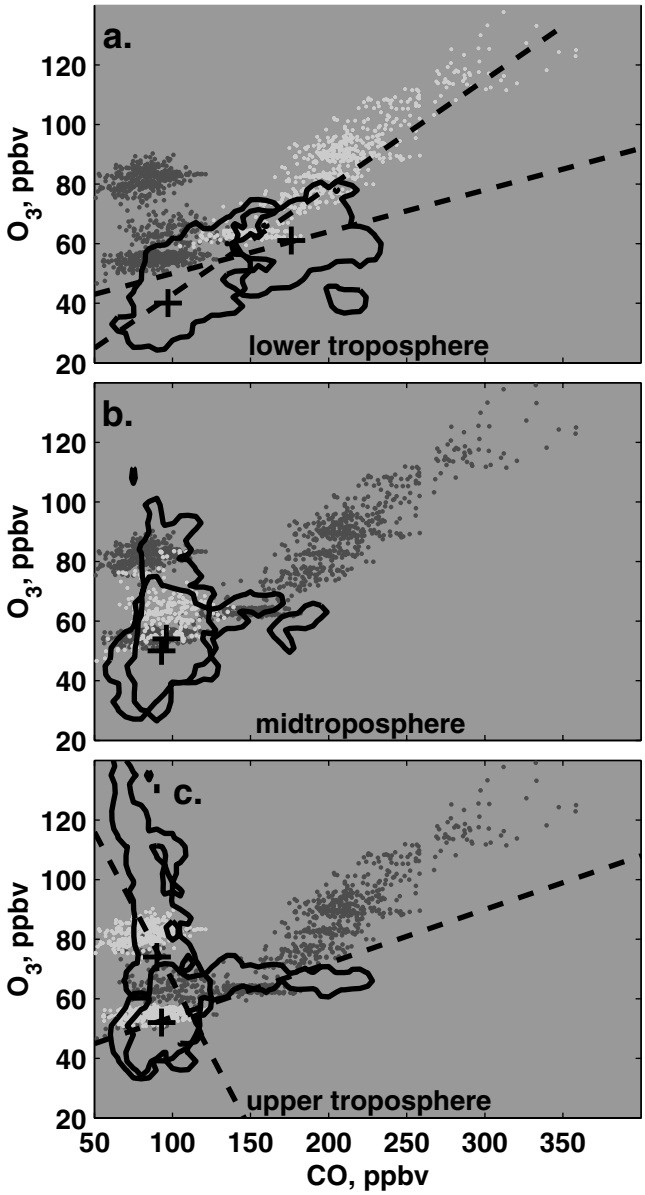

Figure 8. Comparison of 28 August 1993 ozone and CO data (dots) to NARE'96 and NARE'97 data (contours). Outliers were removed from the NARE'96 and NARE'97 data such that the contours encompass 99% of the data points in each group. Data from all flight altitudes on 28 August 1993 are shown (gray dots) with data in the lower, middle, and upper troposphere highlighted (yellow dots). (a) The domains of the NARE'96 and NARE'97 WCB data in the lower troposphere are enclosed by the red and blue contours, respectively; median values for these data sets are also indicated (plus sign). (b) As in Figure 8a except for the DA (blue) and WCB (red) of the midtroposphere from NARE'97. (c) As in Figure 8b except for the upper troposphere. Regression lines (dashed) are drawn through the NARE'96 and NARE'97 data. See color version of this figure at back of this issue.

these data lie outside of the domain of the spring and late summer/early autumn WCB measurements, they fall along the slope of the late summer/early autumn ozone/CO regression line (Figure 8a). As expected, these summertime data have a closer photochemical relationship to the late summer/early autumn data than the spring data, illustrating the conclusion of *Cooper et al.* [2002] that the slope is a robust airstream trace gas signature.

[29] The dry air sampled in the upper troposphere, just above 6 km asl, originated in the dry airstream of the previous cyclone that tracked across eastern North America. Back trajectories and GOES-7 water vapor image loops show that the dry airstream traveled from central Canada to the WNAO on 25 and 26 August. The western extremity circulated back over the United States on 27 August and was pushed out to the region of the flight track on 28 August, ahead of the approaching WCB (Figure 7b). The distribution of ozone and CO in the upper troposphere has more in common with the late summer/early autumn DA distribution than the late summer/early autumn WCB distribution (Figure 8c), indicating a stratospheric influence. There is a good deal of uncertainty in these CO measurements at low mixing ratios [*Buhr et al.*, 1996], but in any event, the CO is low, as would be expected from a stratospheric intrusion, and the ozone (>75 ppbv), hydrocarbon (not shown), and meteorological data all indicate a stratospheric influence. Furthermore, the stratospheric air in this dry airstream produced an enhanced column of ozone in the middle and upper troposphere when it pushed over Bermuda on 27 August 1993 [*Moody et al.*, 1996]. Given that DA fragments or streamers can drift for days in the free troposphere, retaining their chemical signature [*Bithell et al.*, 2000; *Cooper et al.*, 2001a], we do not find unusual the occurrence of a DA fragment above a warm sector.

[30] The ozone/CO distribution of the midtroposphere on 28 August has characteristics of the late summer/early autumn WCB and DA (Figure 8b). This observation is not surprising when one considers that the midtroposphere air mass probably mixed with the DA above and the polluted warm sector below. As discussed in C2002, airstreams of the midtroposphere are most susceptible to mixing with other air masses, blurring the distinction between airstream trace gas signatures.

5. Conclusions

[31] C2002 summarized the characteristic mixing ratios and slopes of their late summer/early autumn composite cyclone with a visual representation of the cyclone conceptual model (see C2002, Figure 10). A similar representation has been produced for the present results, comparing the characteristic ozone (Figure 9) and CO (Figure 10) mixing ratios from late summer/early autumn 1997 and spring 1996. These figures place the results of Table 2 and Figure 3 in the context of the cyclone tracks of Figure 2a. The conceptual cyclone model was partitioned into lower, middle, and upper troposphere layers with the composite cyclone centers representing the average position of the cyclones sampled during each season. The late summer/early autumn composite cyclone is centered just south of Labrador (50°N, 60°W), and the spring composite is centered over the Gulf of Maine (43°N, 68°W).

[32] Several chemical characteristics of midlatitude cyclones become clear in Figures 9 and 10. The most obvious features are the greater ozone and CO median mixing ratios in spring, but much more interesting are the relative relationships of airstream median mixing ratios retained during both seasons. For example, as we work our way from the lower troposphere (PCF) to the upper troposphere (DA) west of the cold front, we find a steady increase of ozone and a steady decrease of CO for both seasons. Focusing on the lower troposphere, we find that the WCB has the most and the PCF has the least ozone in both seasons, while the CCB contains the most CO in both seasons. The one major discrepancy is that during spring ozone decreases from the lower troposphere WCB to the midtroposphere WCB but increases during late summer/early autumn. This is the result of a stronger influence from the marine boundary layer, i.e., less ozone, on lower troposphere measurements during late summer/early autumn. Figure 10 also indicates the sign of the significant slopes of the ozone/CO relationship (those that explain ≈20% or more of the variance). To summarize, photochemical ozone production during late summer/

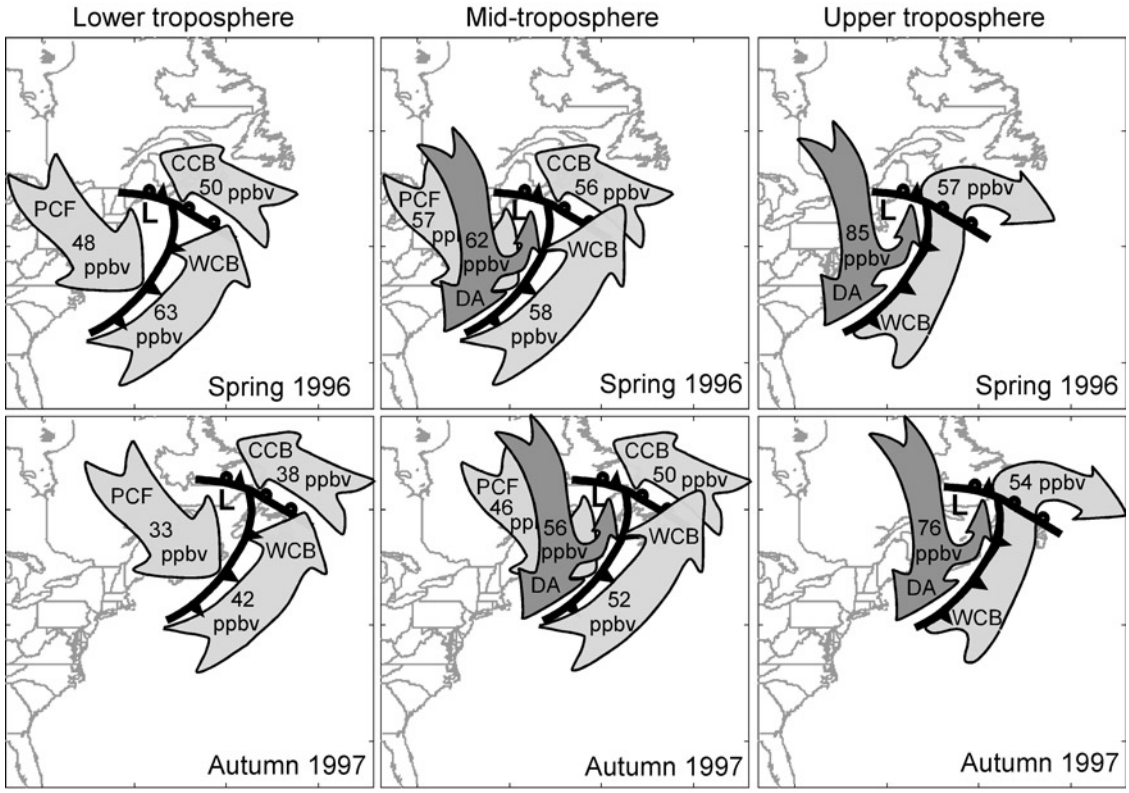

Figure 9. Comparison of the late summer/early autumn 1997 and spring 1996 median ozone values for each airstream (labels are the same as in the text). The center of the low (L) is the mean location of the cyclones that were sampled during that particular season.

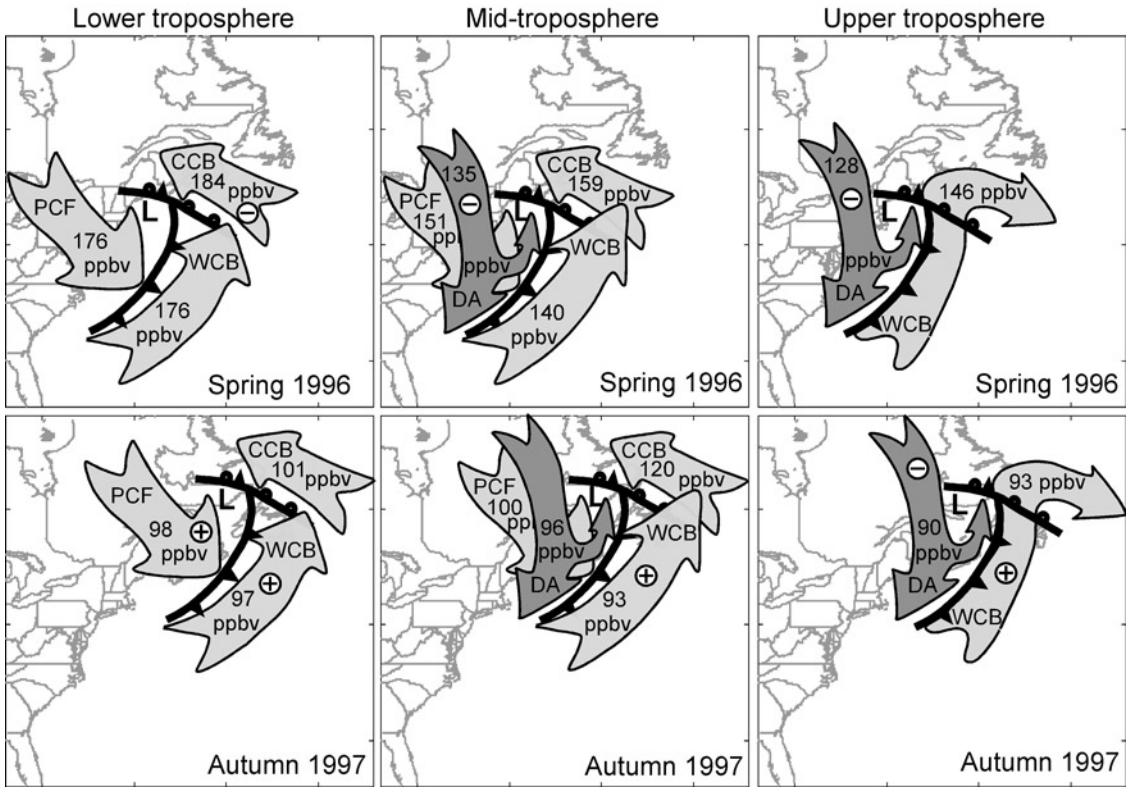

Figure 10. As in Figure 9 except for median CO values. The plus (minus) signs indicate airstreams with significant positive (negative) O_3/CO slopes.

early autumn is associated with the lower troposphere PCF and all levels of the WCB, especially the lower troposphere. During spring, significant photochemical ozone production does not appear to be associated with any airstream at any level, with the lower troposphere CCB associated with photochemical ozone destruction. The negative slopes of the DA indicate STE increases ozone in the middle and upper troposphere. Finally, the more southerly springtime cyclone tracks account for nearly 50% of the increase of lower troposphere CO from late summer/early autumn to spring. The remainder of the variation is due to the seasonal cycle of background CO.

[33] As discussed by C2002, the value of the cyclone conceptual model is that it establishes the fundamental relationships between large-scale chemical transport and midlatitude cyclone structure. The results from the model can also provide critical tests for the output of those chemical transport models (CTMs) with the ability to resolve the structure of cyclone airstreams. We now consider the utility of constructing additional composite cyclones and offer advice for the planning of aircraft campaigns in order to ensure that the major airstreams, and therefore transport paths, are adequately sampled.

[34] The spring and late summer/early autumn composite cyclones capture most of the seasonal variation of ozone and CO. Additional composite cyclones for midsummer and winter would indicate the rate of change of trace gas mixing ratios within airstreams, and composite cyclones for other locations such as the western Pacific would be useful for understanding the chemical composition of the cyclones responsible for trace gas import into North America. As discussed in C2002 and the present manuscript, trace gas relationships such as the ozone/CO or ozone/NO_y slope are the most robust airstream trace gas signatures. However, trends in anthropogenic emission ratios will require that composite cyclones be updated it they are to continue to adequately describe trace gas transport. For example, *Parrish et al.* [2002] show that the CO/NO_x vehicular emission ratio in the US has decreased by nearly a factor of 3 from 1987 to 1999.

[35] The conceptual cyclone model should also prove useful for flight track planning during aircraft intensives. For example, a project interested in sampling photochemically aged air over the eastern United States or WNAO would aim for the WCB, while fresh emissions would most likely be encountered in the PCF, and anyone wishing to sample stratosphere/troposphere exchange events would target the DA. Cyclone airstreams are easily identified from real-time GOES infrared and water vapor imagery, potential temperature surfaces, and back trajectories [*Cooper et al.*, 1998, 2001a], and because they develop over several days, their presence is known at least the day before any given flight. Output from forecast models such as the Eta or MRF can also be used to predict the development and path of airstreams. For example, the WCB appears as a rising conveyor belt when forecast wet-bulb or equivalent potential temperature surfaces are viewed in three dimensions, in conjunction with the forecast position of the high- and low-pressure regions, and the path of the DA can be predicted from cross sections of forecast isentropic potential vorticity. Finer scale features can also be targeted. For example, in a mature occluded cyclone, water vapor imagery reveals that the WCB and DA roll up into a vortex. A flight track bisecting the roll-up in the middle or upper troposphere should encounter trace gas signatures that repeatedly transition between those of the WCB and DA and would be an ideal environment to study the mixing of these two airstreams.

[36] Through the development of the cyclone conceptual model we have attempted to treat the atmosphere as a fluid composed of distinct airstreams with characteristic three-dimensional motions and trace gas signatures. We hope that other researchers will adopt this approach as a means of separating the influences of meteorology, air mass origin, and photochemistry on the chemical composition of the atmosphere. However, we want to emphasize the point that cyclone airstreams are not entirely independent. Midlatitude cyclones form in a sequential manner, one following in the wake of another, each influenced by the airstream remnants of the previous system. For example, when a WCB forms on the western side of surface anticyclones, the DA of the preceding cyclone is descending into the eastern side of the same anticyclone. The DA enriches the midtroposphere above the anticyclone with stratospheric ozone. This air mass subsequently descends as it circulates clockwise around the southern side of the anticyclone [*Danielsen*, 1980; *Thorncroft et al.*, 1993]. Convective mixing on the western side of the anticyclone (WCB) transports the enhanced midtropospheric ozone into the lower troposphere and down to the surface [*Davies and Schuepbach*, 1994; *Cooper and Moody*, 2000]. The result is that a portion of the DA eventually feeds into the WCB immediately upwind. Similarly, the upper tropospheric exit region of the WCB flows alongside the western side of the DA immediately downwind, with subsequent mixing of the two air streams [*Prados et al.*, 1999]. While the mixing of airstreams can confound our efforts to discern airstream trace gas signatures, the prevalence of these systems emphasizes the need to study the atmosphere with equal attention to both chemical and meteorological processes.

[37] **Acknowledgments.** Funding for this research was provided by NOAA awards NA96GPO409 and NA76GPO310 to the University of Virginia. Real-time satellite and meteorological data were provided by UNIDATA internet delivery and displayed using McIDAS software. The CO emission data were created by the EDGAR project (commissioned by the Directorate-General for Environment, Department Air and Energy, of the Dutch Ministry of Housing, Physical Planning and the Environment) and made available through the Global Emissions Inventory Activity (GEIA) website: http://www.rivm.nl/env/int/coredata/geia/index.html.

References

Appenzeller, C., J. R. Holton, and K. H. Rosenlof, Seasonal variation of mass transport across the tropopause, *J. Geophys. Res.*, *101*, 15,071–15,078, 1996.

Bader, M. J., G. S. Forbes, J. R. Grant, R. B. E. Lilley, and A. J. Waters (Eds.), *Images in Weather Forecasting: A Practical Guide for Interpreting Satellite and Radar Imagery*, Cambridge Univ. Press, New York, 1995.

Berkowitz, C. M., K. M Busness, E. G. Chapman, J. M. Thorp, and R. D. Saylor, Observations of depleted ozone within the boundary layer of the western North Atlantic, *J. Geophys. Res.*, *100*, 11,483–11,496, 1995.

Berkowitz, C. M., P. H. Daum, C. W. Spicer, and K. M. Busness, Synoptic patterns associated with the flux of excess ozone to the western North Atlantic, *J. Geophys. Res.*, *101*, 28,923–28,933, 1996.

Bithell, M., G. Vaughan, and L. J. Gray, Persistence of stratospheric ozone layers in the troposphere, *Atmos. Environ.*, *34*, 2563–2570, 2000.

Browning, K. A., and G. A. Monk, A simple model for the synoptic analysis of cold fronts, *Q. J. R. Meteorol. Soc.*, *108*, 435–452, 1982.

Browning, K. A., and N. M. Roberts, Structure of a frontal cyclone, *Q. J. R. Meteorol. Soc.*, *120*, 1537–1557, 1994.

Buhr, M., D. Sueper, M. Trainer, P. Goldan, B. Kuster, F. Fehsenfeld, G. Kok, R. Shillawski, and A. Schanot, Trace gas and aerosol measurements using aircraft data from the North Atlantic Regional Experiment (NARE 1993), *J. Geophys. Res.*, *101*, 29,013–29,027, 1996.

Carlson, T. N., Airflow through midlatitude cyclones and the comma cloud pattern, *Mon. Weather Rev.*, *108*, 1498–1509, 1980.

Carlson, T. N., *Mid-Latitude Weather Systems*, Am. Meteorol. Soc., Boston, Mass., 1998.

Chin, M., D. J. Jacob, J. W. Munger, D. D. Parrish, and B. G. Doddridge, Relationship of ozone and carbon monoxide over North America, *J. Geophys. Res.*, *99*, 14,565–14,573, 1994.

Comrie, A. C., A synoptic climatology of rural ozone pollution at three forest sites in Pennsylvania, *Atmos. Environ.*, *28*, 1601–1614, 1994.

Comrie, A. C., and B. Yarnal, Relationships between synoptic-scale atmospheric circulation and ozone concentrations in metropolitan Pittsburgh, Pennsylvania, *Atmos. Environ.*, *26*(B), 301–312, 1992.

Cooper, O. R., and J. L. Moody, Meteorological controls on ozone at an elevated eastern U.S. regional background monitoring site, *J. Geophys. Res*, *105*, 6855–6869, 2000.

Cooper, O. R., J. L. Moody, J. C. Davenport, S. J. Oltmans, B. J. Johnson, X. Chen, P. B. Shepson, and J. T. Merrill, The influence of springtime

weather systems on vertical ozone distributions over three North American sites, *J. Geophys. Res.*, *103*, 22,001–22,013, 1998.

Cooper, O. R., J. L. Moody, D. D. Parrish, M. Trainer, J. S. Holloway, T. B. Ryerson, G. Hübler, F. C. Fehsenfeld, S. J. Oltmans, and M. J. Evans, Trace gas signatures of the airstreams within North Atlantic cyclones: Case studies from the NARE'97 aircraft intensive, *J. Geophys. Res.*, *106*, 5437–5456, 2001a.

Cooper, O. R., J. L. Moody, T. Thornberry, M. Town, and M. A. Carroll, PROPHET 1998 meteorological overview and air-mass classification, *J. Geophys. Res.*, *106*, 24,289–24,299, 2001b.

Cooper, O. R., J. L. Moody, D. D. Parrish, M. Trainer, J. S. Holloway, T. B. Ryerson, G. Hübler, F. C. Fehsenfeld, and M. J. Evans, Trace gas composition of midlatitude cyclones over the western North Atlantic Ocean: A conceptual model, *J. Geophys. Res.*, *107*, 10.1029/2001JD000901, in press, 2002.

Danielsen, E. F., Stratospheric source for unexpectedly large values of ozone measured over the Pacific Ocean during Gametag, August 1977, *J. Geophys. Res.*, *85*, 401–412, 1980.

Davies, T. D., and E. Schuepbach, Episodes of high ozone concentrations at the earth's surface resulting from transport down from the upper troposphere/lower stratosphere: A review and case studies, *Atmos. Environ.*, *28*, 53–68, 1994.

European Center of Medium-Range Weather Forecasts (ECMWF), *User Guide to ECMWF Products 2.1*, *Meteorol. Bull. M3.2*, Reading, UK, 1995.

Fahey, D. W., and A. R. Ravishankara, Summer in the stratosphere, *Science*, *285*, 208–210, 1999.

Fehsenfeld, F. C., M. Trainer, D. D. Parrish, A. Volz-Thomas, and S. Penkett, North Atlantic Regional Experiment 1993 summer intensive: Foreward, *J. Geophys. Res.*, *101*, 28,869–28,875, 1996.

Galbally, I. E., S. T. Bentley, and C. P. Meyer, Mid-latitude marine boundary-layer ozone destruction at visible sunrise observed at Cape Grim, Tasmania, 41°S, *Geophys. Res. Lett.*, *27*, 3841–3844, 2000.

Komhyr, W. D., Electrochemical cells for gas analysis, *Ann. Geophys.*, *25*, 203–210, 1969.

Komhyr, W. D., R. A. Barnes, G. B. Brothers, J. A. Lathrop, and D. P. Opperman, Electrochemical concentration cell ozonesonde performance evaluation during STOIC 1989, *J. Geophys. Res.*, *100*, 9231–9244, 1995.

Liu, S. C., M. Trainer, F. C. Fehsenfeld, D. D. Parrish, E. J. Williams, D. W. Fahey, G. Hübler, and P. C. Murphy, Ozone production in the rural troposphere and the implications for regional and global ozone distributions, *J. Geophys. Res.*, *92*, 4191–4207, 1987.

Logan, J. A., An analysis of ozonesonde data for the troposphere: Recommendations for testing 3-D models and development of a gridded climatology for tropospheric ozone, *J. Geophys. Res.*, *104*, 16,115–16,150, 1999.

Merrill, J. T., and J. L. Moody, Synoptic meteorology and transport during the North Atlantic Regional Experiment (NARE) intensive: Overview, *J. Geophys. Res.*, *101*, 28,903–28,921, 1996.

Merrill, J. T., J. L. Moody, S. J. Oltmans, and H. Levy II, Meteorological analysis of tropospheric ozone profiles at Bermuda, *J. Geophys. Res.*, *101*, 29,201–29,211, 1996.

Monks, P. S., A review of the observations and origins of the spring ozone maximum, *Atmos. Environ.*, *34*, 3545–3561, 2000.

Moody, J. L., S. J. Oltmans, H. Levy II, and J. T. Merrill, Transport climatology of tropospheric ozone: Bermuda, 1988–1991, *J. Geophys. Res.*, *100*, 7179–7194, 1995.

Moody, J. L., J. C. Davenport, J. T. Merrill, S. J. Oltmans, D. D. Parrish, J. S. Holloway, H. Levy II, G. L. Forbes, M. Trainer, and M. Buhr, Meteorological mechanisms for transporting O_3 over the western North Atlantic Ocean: A case study for August 24–29, 1993, *J. Geophys. Res.*, *101*, 29,213–29,227, 1996.

Moody, J. L., J. W. Munger, A. H. Goldstein, D. J. Jacob, and S. C. Wofsy, Harvard Forest regional-scale air mass composition by Patterns in Atmospheric Transport History, *J. Geophys. Res.*, *103*, 13,181–13,194, 1998.

Novelli, P. C., K. A. Masarie, and P. M. Lang, Distributions and recent changes of carbon monoxide in the lower troposphere, *J. Geophys. Res.*, *103*, 19,015–19,034, 1998.

Olivier, J. G. J., J. P. J. Bloos, J. J. M. Berdowski, A. J. H. Visschedijk, and A. F. Bouwman, A 1990 global emission inventory of anthropogenic sources of carbon monoxide on 1° × 1° developed in the framework of EDGAR/GEIA, *Chem. Global Change Sci.*, *1*, 1–17, 1999.

Oltmans, S. J., et al., Summer and spring ozone profiles over the North Atlantic from ozonesonde measurements, *J. Geophys. Res.*, *101*, 29,179–29,200, 1996.

Parrish, D. D., D. W. Fahey, E. J. Williams, S. C. Liu, M. Trainer, P. C. Murphy, D. L. Albritton, and F. C. Fehsenfeld, Background ozone and anthropogenic ozone enhancement at Niwot Ridge, Colorado, *J. Atmos. Chem.*, *4*, 63–80, 1986.

Parrish, D. D., M. Trainer, J. S. Holloway, J. E. Yee, M. S. Warshawsky, F. C. Fehsenfeld, G. L. Forbes, and J. L. Moody, Relationships between ozone and carbon monoxide at surface sites in the North Atlantic region, *J. Geophys. Res.*, *103*, 13,357–13,376, 1998.

Parrish, D. D., T. B. Ryerson, J. S. Holloway, M. Trainer, and F. C. Fehsenfeld, New directions: Does pollution increase or decrease tropospheric ozone in winter-spring?, *Atmos. Environ.*, *33*, 5147–5149, 1999.

Parrish, D. D., J. S. Holoway, R. Jakoubek, M. Trainer, T. B. Ryerson, G. Hübler, F. C. Fehsenfeld, J. L. Moody, and O. R. Cooper, Mixing of anthropogenic pollution with stratospheric ozone: A case study from the North Atlantic wintertime troposphere, *J. Geophys. Res.*, *105*, 24,363–24,374, 2000.

Parrish, D. D., M. Trainer, D. Hereid, E. J. Williams, K. J. Olszyna, R. A. Harley, J. F. Meagher, and F. C. Fehsenfeld, Decadal change in carbon monoxide to nitrogen oxide ratio in U.S. vehicular emissions, *J. Geophys. Res.*, *107*, 10.1029/2001JD000720, in press, 2002.

Penkett, S. A., and K. A. Brice, The spring maximum in photo-oxidants in the Northern Hemisphere troposphere, *Nature*, *319*, 655–657, 1986.

Penkett, S. A., P. S. Monks, L. J. Carpenter, K. C. Clemitshaw, G. P. Ayers, R. W. Gillett, I. E. Galbally, and C. P. Meyer, Relationship between ozone photolysis rates and peroxy radical concentrations in clean marine air over the Southern Ocean, *J. Geophys. Res.*, *102*, 12,805–12,817, 1997.

Prados, A. I., R. R. Dickerson, B. G. Doddridge, P. A. Milne, J. L. Moody, and J. T. Merrill, Transport of ozone and pollutants from North America to the North Atlantic Ocean during the 1996 AEROCE Intensive Experiment, *J. Geophys. Res.*, *104*, 26,219–26,234, 1999.

Press, W. H., S. A. Teukolsky, W. T. Vetterling, and B. P. Flannery, *Numerical Recipes in Fortran*, The art of scientific computing, 2nd ed., Cambridge Univ. Press, New York, 1992.

Stohl, A., and P. Seibert, Accuracy of trajectories as determined from the conservation of meteorological tracers, *Q. J. R. Meteorol. Soc.*, *125*, 1465–1484, 1998.

Stohl, A., G. Wotawa, P. Seibert, and H. Kromp-Kolb, Interpolation errors in wind fields as a function of spatial and temporal resolution and their impact on different types of kinematic trajectories, *J. Appl. Meteorol.*, *34*, 2149–2165, 1995.

Stohl, A., A one-year Lagrangian "climatology" of airstreams in the Northern Hemisphere troposphere and lowermost stratosphere, *J. Geophys. Res.*, *106*, 7263–7279, 2001.

Thorncroft, C. D., B. J. Hoskins, and M. E. McIntyre, Two paradigms of baroclinic-wave life- cycle behavior, *Q. J. R. Meteorol. Soc.*, *119*, 17–55, 1993.

O. R. Cooper, F. C. Fehsenfeld, J. S. Holloway, G. Hübler, D. D. Parrish, and M. Trainer, NOAA Aeronomy Laboratory, R/AL4, 325 Broadway, Boulder, CO 80305, USA. (ocooper@al.noaa.gov)

J. L. Moody, Department of Environmental Sciences, University of Virginia, Charlottesville, VA 22903, USA.

A. Stohl, Lehrstuhl für Bioklimatologie und Immissionsforschung, Technical University of Munich, Freising, Germany.

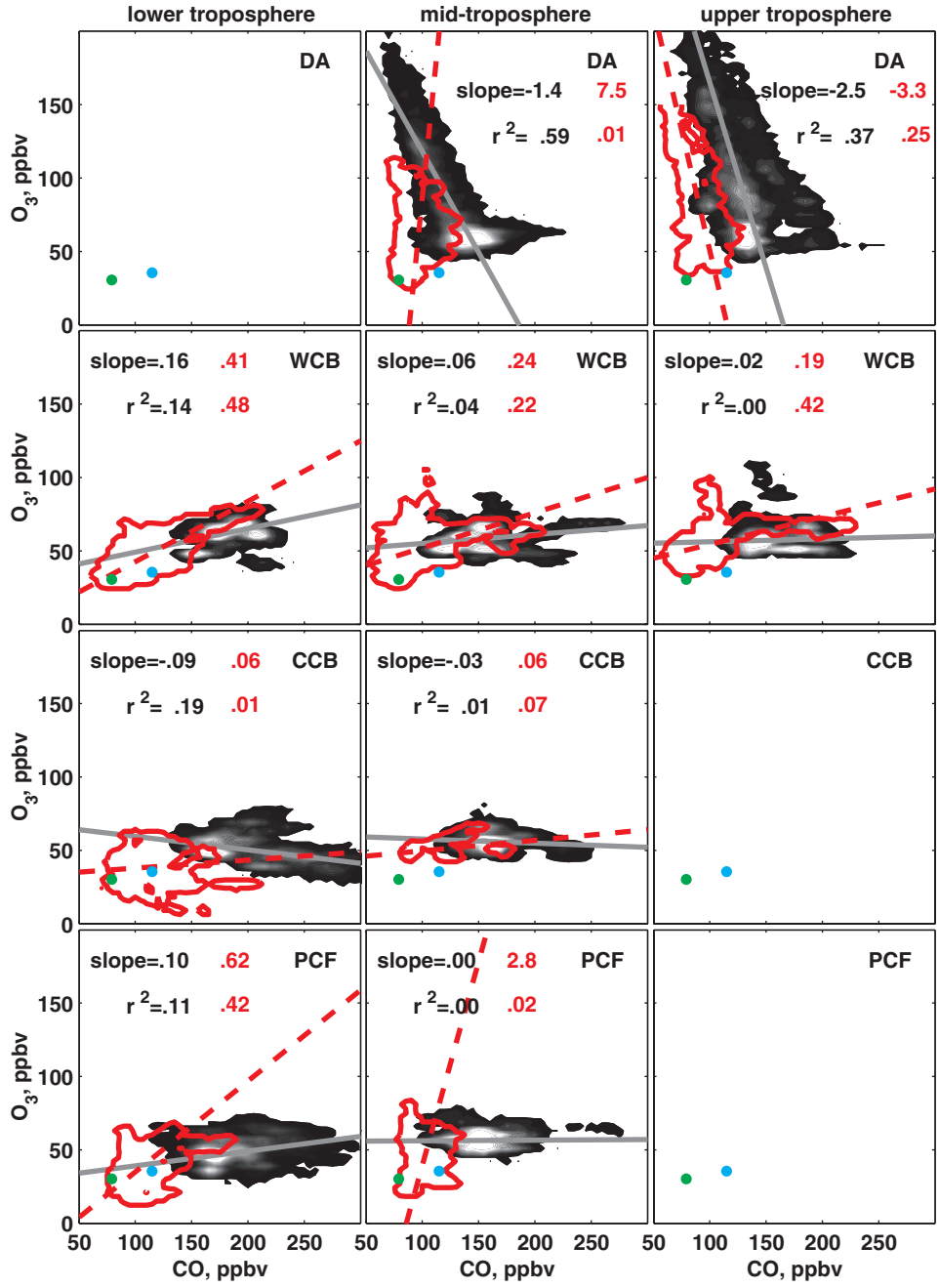

Figure 3. Spring 1996 ozone versus CO for all four airstreams at three levels of the troposphere. The lighter (darker) shading corresponds to relatively higher (lower) data density. The range of the late summer/early autumn 1997 data for each airstream is outlined in red. The linear regression lines for each airstream are shown for spring 1996 (gray lines) and late summer/early autumn 1997 (red dashed lines), with the slope and *r*-squared values labeled in black (spring) and red (late summer/early autumn). Ozone and CO background mixing ratios are shown for spring (blue dot) and late summer/early autumn (green dot).

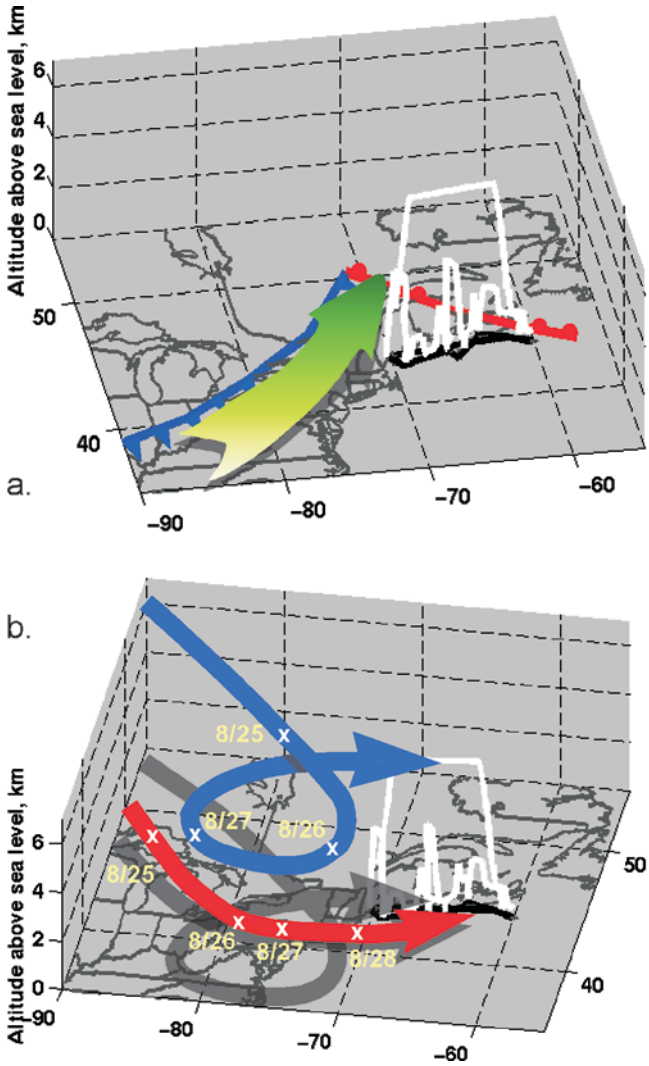

Figure 7. (a) Location of cold and warm fronts, 1200 UTC, 28 August 1993. Flight track is shown in white and the rising green arrow represents the WCB. (b) Back trajectories showing the path of the anthropogenic influenced air mass (red) and stratospheric influenced air mass (blue). The trajectories arrived over the WNAO at 1800 UTC, 28 August; the month and day (m/dd) of the trajectory points at 0000 UTC are shown in white.

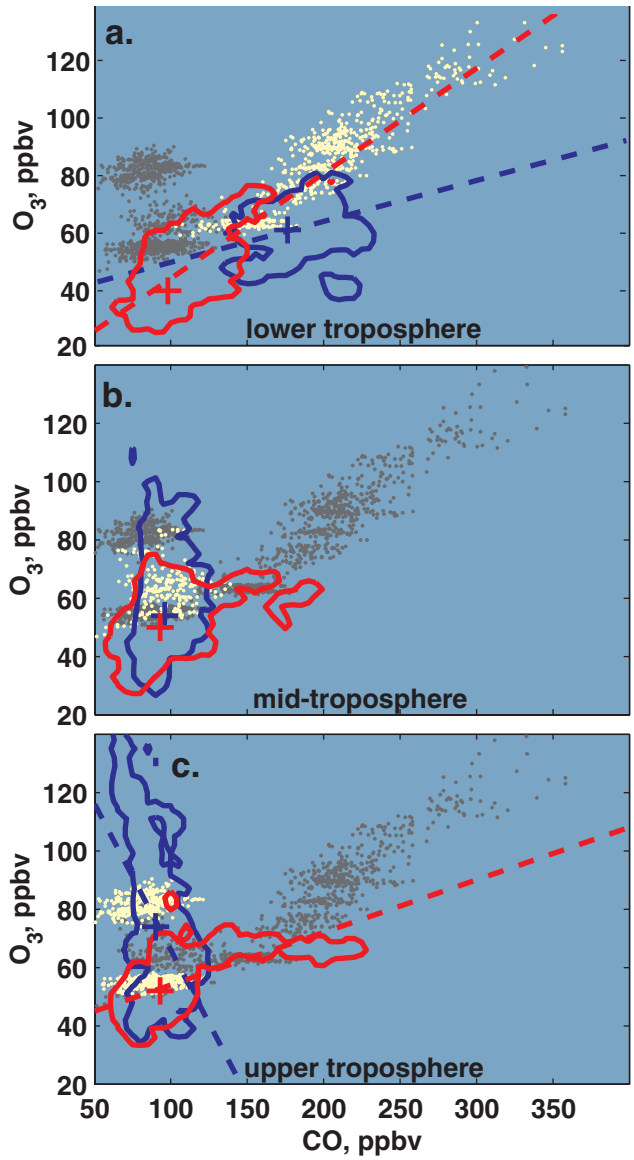

Figure 8. Comparison of 28 August 1993 ozone and CO data (dots) to NARE'96 and NARE'97 data (contours). Outliers were removed from the NARE'96 and NARE'97 data such that the contours encompass 99% of the data points in each group. Data from all flight altitudes on 28 August 1993 are shown (gray dots) with data in the lower, middle, and upper troposphere highlighted (yellow dots). (a) The domains of the NARE'96 and NARE'97 WCB data in the lower troposphere are enclosed by the red and blue contours, respectively; median values for these data sets are also indicated (plus sign). (b) As in Figure 8a except for the DA (blue) and WCB (red) of the midtroposphere from NARE'97. (c) As in Figure 8b except for the upper troposphere. Regression lines (dashed) are drawn through the NARE'96 and NARE'97 data.